Quasar Lenses in the South: searches over the DES public footprint

Adriano Agnello[1], Chiara Spiniello[1,2]

[1]*European Southern Observatory, Karl-Schwarzschild-Strasse 2, 85748 Garching, Germany*
[2]*INAF - Osservatorio Astronomico di Capodimonte, Salita Moiariello, 16, I-80131 Napoli, Italy*

ABSTRACT
We have scanned 5000 deg^2 of Southern Sky to search for strongly lensed quasars with five methods, all source-oriented, but based on different assumptions and selection criteria. We analyse morphological searches based on Gaia multiplet detection and chromatic offsets, fibre-spectroscopic preselection, and X-ray and radio preselection. The performance and complementarity of the methods are evaluated on a common sample of known lenses in the Dark Energy Survey public DR1 footprint. We recovered in total 13 known lenses, of which 8 quadruplets. The method that found the largest number of known lenses is the one based on morphological and colour selection of objects from the WISE and Gaia-DR2 Surveys. We finally present a list of high-grade candidates from each method, to facilitate follow-up spectroscopic campaigns, including two previously unknown quadruplets: WG210014.9-445206.4 and WG021416.37-210535.3.

Key words: catalogues < Astronomical Data bases, Galaxies, galaxies: formation < Galaxies, (cosmology:) dark matter < Cosmology

1 INTRODUCTION

Sizeable samples of gravitationally lensed quasars, spanning a range in redshift, image-separation and mass, are essential to various scientific purposes. However these objects are extremely rare: according to Oguri & Marshall (2010, hereafter OM10), one over $\approx 10^4$ quasars is strongly lensed. One of the first efforts to build a large and well-studied statistical sample of strong gravitational lensed quasars has been made by The Cosmic Lens All-Sky Survey (CLASS, Myers et al. 2003). CLASS has obtained high-resolution radio images from the Very Large Array (VLA, at 8.4 GHz) of over 13000 flat-spectrum radio sources, finding 22 radio-loud lenses. However, in radio lens surveys like CLASS, the redshift distribution of the flat-spectrum sources is poorly constrained (e.g., Muñoz et al. 2003). Only with the advent of the Sloan Digital Sky Survey (SDSS, York et al. 2000, which in its 14th Data Release identified 526,356 quasars (Pâris et al. 2017), has it been possible to construct a large sample of lensed quasars also in the optical (e.g., The Sloan Digital Sky Survey Quasar Lens Search, SQLS, Oguri et al. 2006), beyond the bright lenses identified in older searches.

More recently, thanks to new imaging sky surveys, with wide footprints and sufficient depth and image quality, like ATLAS (Shanks et al. 2015), DES (The Dark Energy Survey Collaboration 2005; The Dark Energy Survey Collaboration et al. 2016) and KiDS (de Jong et al. 2015, 2017), the search for lensed quasars has received new impetus. Nevertheless, to this day, a big portion of the Southern Sky still remains unexplored and the spatial density on sky of known lenses remains much higher at dec.> 0.

In order to fully exploit the wealth of data from different sur-

veys, a suite of new methods to search for lensed quasars (QSOs) have been developed, based on: morphology and visual inspection (Lin et al. 2017; Diehl et al. 2017); spectroscopy (e.g. Oguri et al. 2006; Inada et al. 2012; More et al. 2016); data mining on catalog magnitudes (Agnello et al. 2015; Williams, Agnello, & Treu 2017; Agnello 2017); and variability (Berghea et al. 2017).

As recently quantified by Spiniello et al. (2018, subm.), different search methods are somewhat complementary, as each search relies on different criteria and ancillary information. The application of multiple, state-of-the-art methods over the same footprint then serves two scopes: assessing the role of selection bias in lens samples; and maximizing purity and completeness in lens searches.

With this paper, we perform a comparison study over the footprint covered by the Dark Energy Survey DR1 (DES, The Dark Energy Survey Collaboration et al. 2016; Abbott et al. 2018). Our choice is motivated by three criteria: the DES-DR1 release is public, which ensures reproducibility; its footprint lies mostly in the South, which is still largely unexplored; and the sheer convenience of display from the NCSA DESaccess cutout service, which enabled a swift visual inspection of image cutouts. Magnitudes $W1, W2, W3$ from the Wide-field Infrared Survey Explorer (hereafter WISE; Wright et al. 2010) and from the Gaia space mission (Gaia Collaboration et al. 2016) are given in their native Vega system.

The paper is organized as follows. In Section 2 we describe each of the search methods, and its possible biases. In Section 3 we estimate the performance of each method, in terms of known lens recovery and of new candidates produced over the DES-DR1 footprint. We also provide tables of candidates, to facilitate spectroscopic follow-up, including at least two 'new' quadruplets: WG 210014.9-
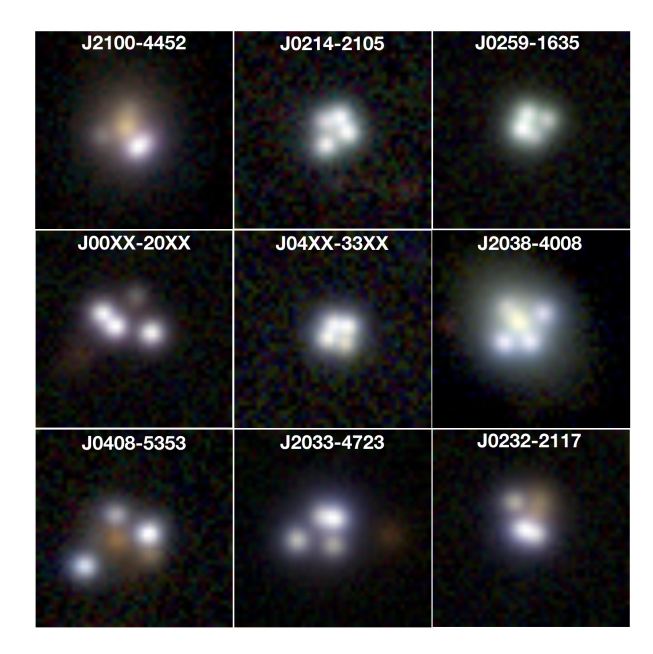
Figure 1. The nine quadruplets found by at least one method in the DES public footprint, with WISE extragalactic colours. The 11.5"×11.5" cutouts are obtained from the DES Data Access page. WG 2100-4452 is a previously unknown quad, and the discovery of WG 0214-2105 has been recently reported by Agnello (2018, RNAAS). WG 00-20 and WG 04-33 have been found independently in STRIDES and are awaiting publication (Schechter & Treu, private comm.). Table 1 gives references for all quadruplets.

445206.4 and WG 021416.37-210535.3 (figure 1). We conclude in Section 4.

2 THE METHODS

We use five different methods, of which: two are mostly morphological and rely on Gaia multiplet detection or chromatic offsets; one is based on spectroscopic preselection from fibre-spectroscopic surveys; and two are based on radio and X-ray preselection.

The searches are structured similarly: a first step of *object preselection*, based on shallow cuts on catalog magnitudes and colours; a second step of *target* selection, still based on catalog entries; and a final step of *candidate* selection, through visual inspection of image cutouts. For the sake of convenience, the DES-DR1 public cutout service was used. However, in its current version, it properly displays between 50% and 70% of the cutouts that are produced. For this reason, the final numbers of candidates given in this paper should be taken as purely indicative, and a significant number of quasar lenses may still be found among the systems that were not properly displayed.

2.1 BaROQuES: Blue and Red Offsets of Quasars and Extragalactic Sources

The Gaia mission had $\approx 2''$ image resolution in DR1 and $\approx 0.5''$ in DR2, which enables the recognition of multiple images in lensed quasars that are otherwise not deblended by the image-processing pipelines of ground-based surveys. The search of quasar lenses in DES through Gaia-DR1 multiplet recognition has already been made within STRIDES (Agnello et al. 2017). However, not all known lenses are deblended into multiple `source` entries in Gaia-DR1 (e.g. Agnello et al. 2017).

For systems that are not Gaia multiplets, we can still use the accurate astrometry of Gaia to compare chromatic shifts in image centroids among different surveys, under the hypothesis that lenses have non-negligible offsets due to the different contributions of source and deflector in different bands. To this aim, we consider objects that are bright enough to have positions in the 2MASS catalog, and consider their 2MASS-Gaia offsets. Matters are slightly complicated, due to atmospheric differential refraction (ADR) and the choice of astrometric calibrators for each survey. Recent searches based on chromatic offsets (Lemon et al. 2018) relied on SDSS-vs-Gaia solutions, calibrated on astrometric reference stars, and had abundant contamination from isolated (unlensed) quasars. This is due to the different colours of quasars and astrometric stars, which can result in $\approx 0.3''$ offsets due to ADR (with typical ≈ 20 deg Zenith angles of ground-based surveys).

We resolve this by means of field-corrected offsets, using our own BaROQuES scripts[1], as follows. First, we work with a sample of quasar-like objects, selected in WISE as:

$$W1 - W2 > 0.35 - \sqrt{(\delta W1)^2 + (\delta W2)^2} \,, \tag{1}$$

$$W1 - W2 > 0.2 + \sqrt{(\delta W1)^2 + (\delta W2)^2} \,, \tag{2}$$

$$W2 - W3 > 2.1 + \sqrt{(\delta W2)^2 + (\delta W3)^2} \,, \tag{3}$$

$$W1 < 17 \,, \ W2 < 15.6 \,, \ W3 < 11.8 \,. \tag{4}$$

Then, for each given object we examine a surrounding patch of $1.0 \times 1.0 \text{deg}^2$, containing ≈ 40 QSO-like neighbours. We then compute the average offsets between their 2MASS and Gaia coordinates $\delta x = -\cos(\text{dec.})\delta\text{r.a.}$, $\delta y = \delta\text{dec.}$, subtract them from the offsets of the given object, and retain it only if this corrected offset is between $0.27''$ and $1.8''$. This ensures that known lenses are recovered, and chance alignments of quasars with other objects are safely rejected. By working directly with WISE-selected quasar-like objects, this problem is bypassed and isolated quasars are automatically rejected.

When applied to the Southern Galactic Hemisphere, with $b < -20$ and -70<dec<7, this gave $\approx 6 \times 10^4$ objects, of which 31381 singlets and 770 multiplets in the DES-DR1 footprint.

2.2 Gaia-DR2 Multiplets

The nominal resolution of Gaia has improved from $2''$ (DR1) to $0.4''$ (DR2), so a simple upgrade consists in searching again for Gaia-DR2 multiplets corresponding to WISE sources. There is indeed some improvement from DR1 to DR2: out of the $\approx 6 \times 10^4$ Gaia-DR1 singlet 'baroques' from above, a match with DR2 gave 2149 multiplets, of which 134 with more than two `source` entries.

However, some candidates and small-separation lenses from DR1 have disappeared in the passage to DR2 (e.g. the lens WGD0508, Agnello et al. 2017). The same has been noticed in Spiniello et al. (2018, subm) on a smaller footprint (KiDS-DR3, 450 deg^2). In general, the Gaia-specific deblending does not seem to have a well defined behaviour with separation and flux-ratios, as some small-separation lenses are recognized as multiplets while larger-separation lenses correspond to Gaia singlets (e.g. WGD0150, WGD0245; Agnello et al. 2017).

In order to make additional progress over the searches in Gaia-DR1, we also relaxed the preselection photometric criteria. From a

---

[1] Blue and Red Offsets of Quasars and Extragalactic Sources, available upon request, `https://github.com/aagnello` .

WISE search, we selected extragalactic objects as

$$W1 - W2 > 0.2 + \sqrt{(\delta W1)^2 + (\delta W2)^2} \,, \tag{5}$$
$$W1 < 17 \,, \ W3 < 12.4 \tag{6}$$

basically excluding stars ($W1 - W2 \approx 0$) and fainter objects with unreliable catalog magnitudes. This gave $O(10^6)$ objects with Galactic Latitude $b < -15$. Of these, $O(10^5)$ are recognized as multiplets in Gaia-DR2. However, many are clustered towards the Galactic disc and the Magellanic Clouds, which can be explained with the line-of-sight alignment of quasars with stars. In order to exclude most quasar-star pair contaminants, we then impose a threshold on the ratio Σ_m/Σ_s between multiplet and singlet densities. For the Gaia doubles, we retain only objects in regions where $\Sigma_m/\Sigma_s < 0.2$; for Gaia triplets and quadruplets, we relax it to $\Sigma_m/\Sigma_s < 0.3$. After the overdensity threshold cuts, ≈ 17000 multiplets remain, of which 8146 lie in the DES-DR1 public footprint.

2.3 Spectroscopic Surveys

Some of the longest known quasar lenses, such as e.g. Q0957+561 (Walsh, Carswell, & Weymann 1979) and lenses from the Hamburg-ESO survey (Wisotzki et al. 1996), were found in wide-field, prism spectroscopic surveys. Over the last decade, searches in the SDSS and BOSS (Inada et al. 2012; More et al. 2016) relied on samples of objects that were classified as quasar based on fibre spectroscopy. Also, some lenses recently found in the DES (Ostrovski et al. 2017; Agnello et al. 2017) had pre-existing fibre spectra in the Anglo-Australian Observatory databases, where they had been targeted as quasars or galaxies and not recognized as lenses, due to low image resolution.

For this reason, we examined two surveys with moderate depth and uniform coverage over large areas in the Southern Hemisphere: the six-degree field galaxy survey (6dFGS, Jones et al. 2004) and the 2QZ (Boyle et al. 2000). These were also based on different preselection cuts, based on optical cuts in all-sky surveys of moderate depth, focusing on galaxy-like (6dFGS) or quasar-like (2QZ) objects. In this sense, then, they are also complementary to the WISE criteria that we have used in our photometric searches.

We restrict these samples to objects with pipeline redshifts $z_s > 0.5$, as expected from simulated samples (OM10) and our benchmark of CASTLES/SQLS known lenses. This gave 1625 objects from the 6dFGS and 7147 from 2QZ, over the DES footprint.

2.4 X-Ray

Quasars can also be targeted in X-ray emission, due to lower dust attenuation in that spectral range. The recently vetted cross-match (Salvato et al. 2018) the ROSAT all-sky survey (Boller et al. 2016) and XMMslew survey (Georgakakis & Nandra 2011) with WISE then provides an alternative preselection of possible candidates. Some lenses discovered in ROSAT are indeed known, such as RXJ0911.4+0551 (Bade et al. 1997), RXJ0921+4529 (Muñoz et al. 2001), and RXJ1131-1231 (Sluse et al. 2003). A fainter lens, CY2201-3201 (Castander et al. 2006) was found in the Chandra deep fields.

We then used the publicly available cross-match tables[2] to pre-select X-ray objects. Also in this search, we excluded possible

---

[2] http://www.mpe.mpg.de/XraySurveys/2RXS/

stars with the same cuts as above. This yielded 13547 cutouts from ROSAT-WISE, and 2294 from XMM-WISE.

2.5 Radio

Similarly to X-ray preselection, radio searches are less affected by reddening and by the presence of a foreground galaxy. As a consequence, they bypass the colour selection that can affect optical or IR searches. Indeed, quasar lens discoveries in the past have benefited from hemispheric surveys like the Parkes-MIT-NRAO survey (Griffith & Wright 1993) and dedicated observations by the CLASS (Myers et al. 2003) and J-VLA (King et al. 1999) searches.

Here, we use the Sydney University Molonglo Sky Survey (SUMSS Mauch et al. 2003), covering the Southern Hemisphere down to ≈ 10 mJy at 0.84 GHz. We match the catalog with WISE, using a nearest-neighbour match with $10''$ search radius, and retained extragalactic objects as above. This resulted in 38204 cutouts within the DES-DR1 footprint.

3 PERFORMANCE

The performance of each method can be quantified in different ways. One metric is given by completeness and purity with respect to previous searches. Another possibility is the number of candidates that are produced by each method over the same footprint. The final evaluation of performance is the purity of the candidate samples, once spectroscopic follow-up is performed. The candidates presented in this paper are still awaiting spectroscopic confirmation, and published samples of lenses and contaminants over the DES footprint are still too small to build meaningful statistics. Then for the scope of this paper, we discuss the recovery of known lenses over DES-DR1, and properties of candidate samples from different searches.

3.1 Known Lenses, and the DES subsample

Table 1 lists the known lenses recovered over the DES-DR1 footprint. Five lenses are two image systems, and eight are (at least) quadruplets. Two of them (WG 04-33, WG 00-20) have been found independently within the STRIDES collaboration (Schechter & Treu, private comm.) and are awaiting publication. For this reason, we list them as known lenses, with partially obscured coordinates, instead of as new candidates from our searches. The discovery of WG 0214-2105 has been recently reported by Agnello (2018, RNAAS).

The recovery statistics of known lenses in Gaia-DR2 is slightly better than for Gaia-DR1 (e.g. Agnello 2017). We quantify this through a list of 214 known quasar lenses and pairs collected from the SQLS (Inada et al. 2012) and CASTLES databases, consistently with previous work (Williams, Agnello, & Treu 2017). Of these, 43 are missing from Gaia-DR2. Of the 171 that are detected, 124 are resolved in two sources, 15 into three sources, and six into four sources. Small-separation lenses are absent in Gaia-DR2, because of a sharper cutoff at $\approx 0.5''$ separations in the DR2 catalog. These include also lenses that were found thanks to Gaia-DR1 (e.g. WGD 0508, Agnello et al. 2017).

3.2 Candidates

Visual inspection of targets from the above methods resulted in: 17 BaROQuES in Gaia-DR1 vs 2MASS, of which 5 Gaia multiplets;
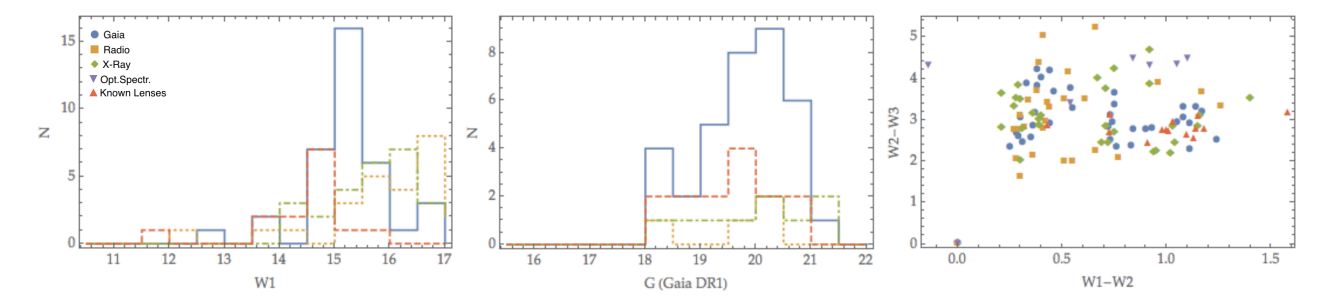
Figure 2. Magnitude and colour distributions of candidates and known lenses. *Left:* $W1$−magnitude distribution for Gaia candidates (blue), radio candidates (orange, dotted), X-ray candidates (green, dot-dashed) and known lenses (red, dashed). *Middle:* G−magnitude distribution, with the same colour coding. *Right:* colours $W1 - W2$ vs $W2 - W3$, same colour coding (and markers) as in the first panel. BaROQueS and Multiplets are grouped, because they are both based on Gaia. Red triangles represent the known lenses recovered by the five searches.

Table 1. Known lenses in the DES-DR1 public footprint recovered by the different search methods of Section 2. Magnitudes are from WISE and Gaia-DR1 and given in the Vega system. The first 6 systems in the table are the known quadruplets, whose cutouts are also shown in Figure 1. Here, W2MG1 denotes 2MASS-vs-Gaia chromatic offsets (see Section 2.1), and 'mult' or 'sing' marks objects that correspond to Gaia multiplets or singlets, respectively.

object	$W1$	$W2$	$W3$	G	methods	reference
J00XX-20XX	14.56±0.03	14.01±0.04	10.76±0.10	19.21	GaiaDR2mult	Lemon et al (in prep.)
J021416.37-210535.3	15.11±0.03	14.68±0.06	11.82±0.24	19.80	GaiaDR2mult	Agnello (2018, RNAAS)
J023233.16-211725.7	14.02±0.03	12.99±0.03	10.06±0.05	18.93	XMMslew	Wisotzki et al. 1999
J025942.86-163543.0	13.86±0.03	13.13±0.03	10.03±0.05	19.22	W2MG1sing	Schechter et al. 2018
J04XX-33XX	13.85±0.03	12.71±0.02	9.94±0.04	20.22	W2MG1mult,GaiaDR2mult	Anguita et al. (2018 subm.)
J040821.63-535358.9	14.08±0.02	13.17±0.02	10.75±0.06	19.63	GaiaDR2mult	Lin et al. 2017
J203342.12-472343.9	13.49±0.03	12.34±0.03	9.25±0.04	17.98	W2MG1mult,GaiaDR2mult	Morgan et al. 2004
J203802.69-400813.9	11.43±0.02	10.25±0.02	7.49±0.02	19.44	W2MG1mult,GaiaDR2mult,6dFGS	Agnello et al 2017/8
J011557.37-524423.4	14.49±0.03	13.36±0.03	10.82±0.11	20.40	GaiaDR2mult	Agnello et al 2015
J014632.87-113339.2	14.17±0.03	13.08±0.03	10.45±0.06	18.39	W2MG1mult,GaiaDR2mult	Agnello et al 2017/8
J023527.42-243313.8	14.00±0.03	13.02±0.03	10.29±0.05	18.12	W2MG1mult,GaiaDR2mult	Agnello et al 2017/8
J051410.90-332622.4	13.29±0.03	11.71±0.02	8.54±0.02	17.80	HE, RASS	Gregg et al 2000
J202139.38-411557.9	14.17±0.03	13.17±0.03	10.44±0.07	19.27	W2MG1mult,GaiaDR2mult	Agnello et al 2017/8

23 candidates from Gaia-DR2 multiplets; 7 candidates from fibre-spectroscopy (3 from 6dFGS and 4 from 2QZ); 30 candidates from X-ray preselection, of which 29 from ROSAT; and 29 candidates from SUMSS. The full lists of high-graded candidates are provided in Tables A1 and A2, divided by search method. We list their names (J2000 coordinates), as well as their WISE (W1,W2,W3) and Gaia-DR1 (G) magnitudes.

Figure 2 shows the colour and magnitude distributions of the candidates. Different colours and markers represent the different methods through which the candidates have been identified. Known lenses are plotted in red (dashed in the magnitude histograms, triangles in the colour-colour plot). Gaia-selected candidates extend the regime of known lenses towards fainter magnitudes, still with a cutoff at the faint end due to noisy WISE magnitudes and the drop in Gaia completeness at $G \approx 20$. X-ray and radio selected candidates populate the faint end of the magnitude distribution, with few objects corresponding to optical detections in Gaia.

Two main clusters of systems are visible in the WISE colour-colour plot: objects with high $W1 - W2$, compatible with QSO-dominated photometry, and systems with lower $W1 - W2$, compatible with galaxy-dominated photometry. Systems with low W1-W2 (left-most panel) mostly have $W3 \geqslant 11.8$, which is the threshold where WISE magnitudes become unreliable. There is a prevalence of radio-selected objects in the galaxy-dominated clump, whereas

X-ray and Gaia selected systems are evenly distributed. Known lenses are mostly associated to the QSO-dominated regime.

Candidates selected from each method are shown in Figures 3 and 4. All methods produce sensible results upon visual inspection, albeit with a predominance of high-grade candidates from the Gaia searches. Some candidates (mostly from SUMMS and spectroscopic surveys) may be lenses with bright deflectors, or mergers of compact narrow-line galaxies at lower redshift. With the depth ($i \approx 22.5$) and image resolution of Pan-STARRS and DES-DR1 ($\approx 0.26''/\text{px}$, $\approx 1''$ seeing), these contaminants are still present in candidate samples.

3.3 Quadruplets

Due to their higher number of images, with respect to doubles, quadruplets yield more constraints on the deflector potential and stellar mass fraction, and for this reason they are especially valued probes of cosmography (e.g. Refsdal 1964; Blandford & Narayan 1992; Witt, Mao, & Keeton 2000; Suyu et al. 2013; Treu & Marshall 2016; Bonvin et al. 2017) and microlensing studies (e.g. Schechter et al. 2014).

A quadruplet configuration requires an even closer alignment of source and deflector than doubles. The fraction of quadruplets in statistically-complete quasar lens samples is esti-

W2MG1

GaiaDR2-Multiplets

Figure 3. Examples of candidates found in Gaia DR1 and DR2, with WISE preselection. W2MG1 denotes WISE objects with acceptable offsets between their 2MASS and Gaia-DR1 catalog positions, with recomputed astrometry from our BaROQuES scripts.

mated at 14% (OM10). The two quadruplets found within this search, WG210014.9-445206.4 and WG021416.37-210535.3, correspond to Gaia-DR2 triplets and are already shown in Figure 1. Most of the other candidates, except some radio-selected and spectroscopically-selected candidates, are doubles. We emphasize that, while WG 0214-2105 requires little follow-up for confirmation, in principle the chromaticity in WG 2100-4452 requires a final step of spectroscopic confirmation to secure its lensing nature.

Two quadruplets found in this search, at J04-33 (Anguita et al., subm.) and J00-20 (Lemon et al., in prep.) have also been discovered independently within the STRIDES[3] collaboration (Schechter & Treu, private comm.). Even though they were found *blindly* by our search, using exclusively public datasets, and so would be legitimate candidates in the framework of this paper, we prefer to list them as known lenses with partially obscured coordinates, in view of publication by other teams.

3.4 Completeness

The statistics of quadruplets is also an indication of completeness in a quasar lens search, relative to the number of objects at preselection. A 'demanding' quasar preselection (e.g. $W1 - W2 >$

$0.55 + \sqrt{(\delta W1)^2 + (\delta W2)^2}$, Agnello et al. 2017) produces ≈ 40 objects per square degree, which (adopting OM10 lensing rates) gives ≈ 20 lenses over the DES footprint, of which $\approx 2.8 \pm 1.67$ should be quads. A WISE preselection like the ones in this paper produces 110 ± 10 objects per square degree, and should result in 7.7 ± 0.7 quadruplets over the DES footprint. The current number of 9 quads (partly known and partly new) suggests that the steps of target and candidate selection are reasonably complete.

In order to find more quads, then, the main bottleneck is that of colour preselection. Searches with hybrid, optical-IR colours would allow one to relax the WISE extragalactic cuts, but in this exploration we preferred to use the DES-DR1 only for the final stage of visual inspection, in order not to impose a prejudice on the optical colours of lensed quasars upon our searches.

4 DISCUSSION

We have discovered two previously unknown quadruplets, WG210014.9-445206.4 and WG021416.37-210535.3. We have independently discovered another two (J00-20, J04-33) that are currently awaiting publication by the STRIDES collaboration, which we prefer to list among other known lenses in the DES footprint.

The use of five different selection methods, over spectral ranges ranging from X-ray to radio through optical, has resulted in 100 quasar lens candidates over the DES-DR1 public footprint. The number of quadruplets found in this paper suggests that the searches

---

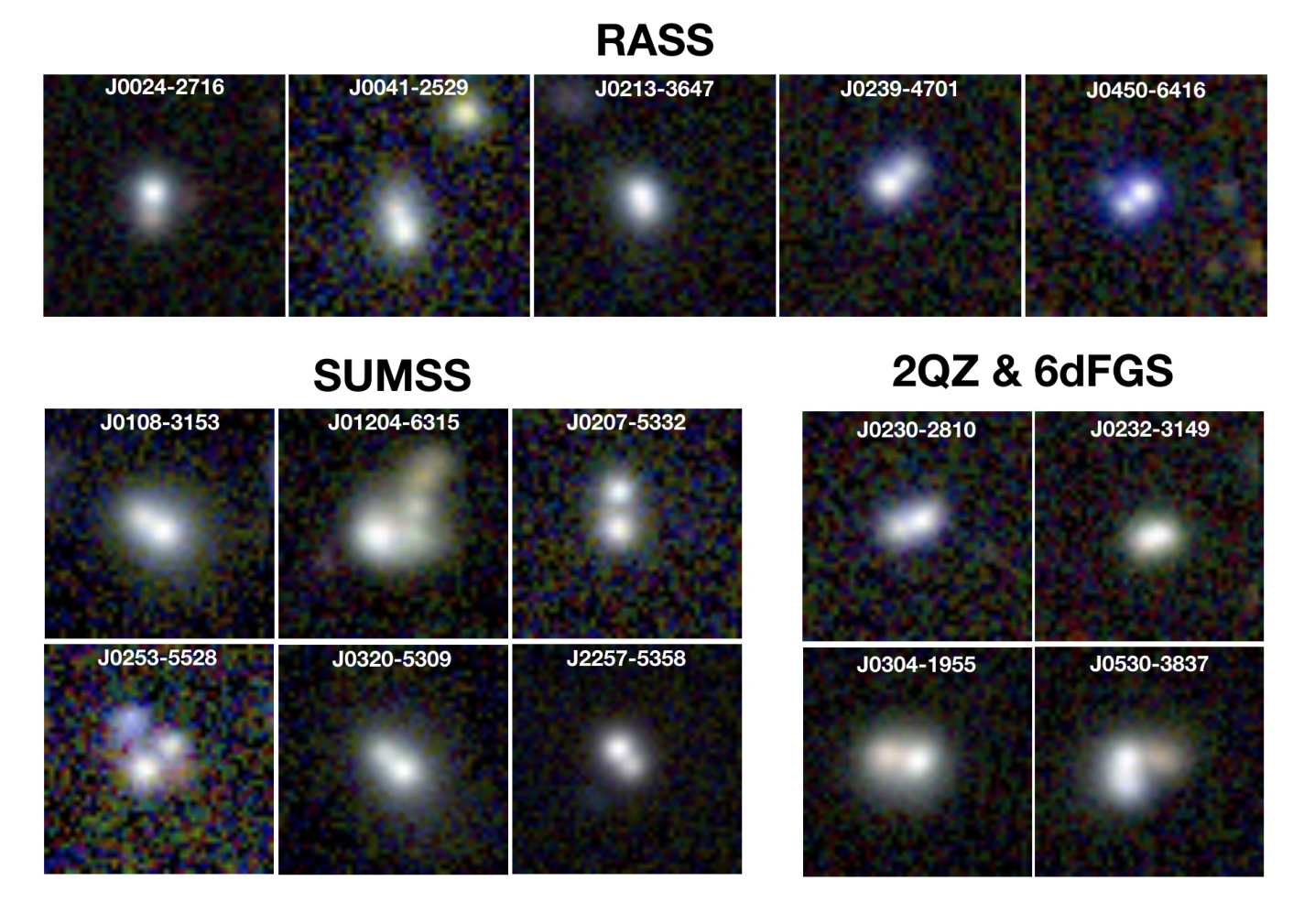[3] STRIDES is a broad external collaboration of the Dark Energy Survey, `strides.astro.ucla.edu`

Figure 4. Examples of candidates found with spectroscopic (2QZ, 6dFGS), radio (SUMMS) or X-Ray (ROSAT, XMMslew) surveys.

are reasonably complete, and that the main bottleneck is the very first step of object preselection.

All of the searches involved a step of WISE pre-selection, imposing some loose cuts on colours in order to isolate extragalactic objects, and results in two main clusters of candidates based on whether their photometry is quasar-dominated or galaxy-dominated. Due to the current capabilities of the DESaccess server with large cutout queries, approximately two thirds of targets in the DES-DR1 footprint were properly displayed, so another ≈ 50 candidates may be still awaiting discovery.

4.1   Deeper and Sharper WISE preselection

At the stage of WISE preselection, we are currently limited by two factors: the uncertainties in $W1, W2, W3$ magnitudes; and image resolution. First, the searches are cut at $W1 < 17$ and $W2 < 15.6$ since the magnitudes of fainter objects are more affected by Earth-shine and become quickly unreliable. Second, the $\approx 6''$ (FWHM) image resolution of WISE prevents any comparison of the mid-IR colours of different components, which at these wavelengths should be unaffected by reddening and microlensing and would then make a powerful selection criterion.

Forced photometry upon WISE cutouts, using object positions from sharper surveys (like Gaia or the DES), would alleviate these issues and enable a deeper and sharper search, maximizing the in-

formation content of WISE. This, of course, requires that multiple components are identified by the optical surveys, and that their separation is wide enough ($\gtrsim 2.5''$) so that the magnitudes inferred through forced photometry are reliable. From a re-reduction (Meisner et al. 2017) and forward modeling of WISE/NeoWISE survey tiles, forced-photometry magnitudes are currently available for the SDSS (Lang et al. 2016) and the DECaLS (Dey et al. 2018) footprints, covering 'Northern' declinations above -20 degrees. By using Gaia multiplets as a base for forced photometry, a search based on mid-IR (deblended) colours may be extended to the whole sky. However, the completeness of the resulting sample would be ill characterized, as the current releases of Gaia fail to properly deblend lenses (e.g. WGD 0150, WGD 0245, Agnello et al. 2017) that are clearly deblended into multiplets by other surveys such as the DES.

Another way of increasing depth and imaging resolution, in the BaROQuES approach, would be to replace 2MASS with deeper surveys, such as UKIDSS (Warren et al. 2007) or VHS (McMahon et al. 2013). However, their sky coverage is not homogeneous, whereas 2MASS covers the whole sky, and their application to a DES search is of limited use since their overlap with the DES footprint is only partial. Wile UKIDDS is primarily a Northern Hemisphere survey,

VHS was planned to cover the whole Southern Hemisphere, but[4] it is mostly limited to $-20 \leqslant$ dec. < 0 and $-50 \leqslant$ dec. < -40, and not homogeneously.

4.2 Towards LSST

While near-IR surveys (e.g. VHS, UKIDSS, VHS) are ideally suited for chromatic offsets, due to the different colours of sources and deflectors, optical surveys can be a valid alternative. Lemon et al. (2018) have successfully used SDSS instead of 2MASS, and our BaROQuES procedures have been applied with success to the KiDS-DR3 450 deg^2 footprint (Spiniello et al. 2018, subm.). In the near future, LSST (SV due 2022, SciOps due 2023) will enable the extension of these searches to the whole Southern Hemisphere.

Despite the deluge of multi-epoch data from the full survey, the foreseen volume of nightly observations is still manageable, and automated procedures for chromatic offsets can be run on a nightly basis. This pipeline-oriented approach will then bring the discovery of lensed quasars to the same, high-cadence pace of transient discoveries. Ideally, chromatic offsets can be computed among different bands within LSST, without the recourse to external surveys like Gaia or 2MASS, provided nightly data are deep enough to guarantee robust astrometry in separate bands.

4.3 Gaia DR3, DR4 and Euclid

The DR2 of Gaia provided additional information over DR1, such as blue and red pass-band magnitudes ($G_{\rm bp}$, $G_{\rm rp}$), as well as parallax and proper motion, for sources towards the bright end. It has a safety cutoff at $\approx 0.5''$ nearest neighbours, which prevents the discovery of small-separation lenses through multiplet recognition but may be reassessed in future releases. The pipeline proper motions of known lenses are not necessarily small (Spiniello et al. 2018, subm.), and colours from $G_{\rm bp}$, $G_{\rm rp}$ can only be used for the brighter candidates.

The final Gaia-DR4 release, due in 2020, is planned to provide low-resolution spectra of all detected Gaia sources. This would provide a selection of lens candidates based uniquely on Gaia, by-passing broad-band colour selection, through the detection of emission lines from the source quasars. This approach closely resembles the Hamburg-ESO strategy of isolating quasars based on their low-resolution spectra and following them up with higher imaging resolution, but it would be applied over the whole sky and down to fainter magnitudes.

Beyond the spectroscopic and multiplet selection in Gaia, an obvious step forward will be the Euclid space mission (Laureijs et al. 2010). The lessons learnt from the Gaia pipelines, in deblending objects into multiple sources and extracting spectra, will be essential to the development of lens searches within Euclid. In these all-sky perspectives, significant improvement is needed on the final stage of candidate selection, whether it is based on direct cutout modeling or direct visual inspection. Dedicated deblenders are being developed to this purpose (e.g. Chan et al. 2015; Schechter et al. 2018), but they still require manual 'tuning' to the specifics of each survey, and a considerable amount of visual inspection.

4.4 Beyond ROSAT: eROSITA

The optical and X-ray choices of preselection are quite complementary. On the one side, X-ray selected sources populate the faint end of the WISE and Gaia magnitude distribution, and sometimes miss Gaia `source` counterparts. On the other, only two of the known lenses in the DES are detected by our ROSAT-WISE search, and in general X-ray selected lenses are a minority among the CASTLES sample.

In the near future, eROSITA (Merloni et al. 2012) promises a ≈ 20 deeper coverage than ROSAT in the soft X-ray, and the first ever all-sky survey in the hard X-ray. The forecast of ≈ 100 detected objects per square degree, over the four-year span of the survey mission, is comparable to the WISE extragalactic selections used in this paper, and based on completely independent spectral signatures. In particular, from the expected number of active galactic nuclei (AGN) with redshift $1 < z_s < 3$ and the OM10 estimates, eROSITA should detect ≈ 120 lensed quasars over its 30000 deg^2 footprint, a quarter of which would have an obscured AGN as a source.

---

[4] Based on the final release (2018-02-09) by the ESO Archive Group, https://www.eso.org/qi/catalog/show/217, see 'Description' for warnings on catalog usage and missing entries.

[5] See https://des.ncsa.illinois.edu/thanks for full list of Collaborating Institutions.

Inter-American Observatory, National Optical Astronomy Observatory, which is operated by the Association of Universities for Research in Astronomy (AURA) under a cooperative agreement with the National Science Foundation.

REFERENCES

Abbott T. M. C., et al., 2018, arXiv, arXiv:1801.03181

Agnello A., Kelly B. C., Treu T., Marshall P. J., 2015, MNRAS, 448, 1446

Agnello A., et al., 2015, MNRAS, 454, 1260

Agnello A., 2017, MNRAS, 471, 2013

Agnello A., et al., 2017, arXiv, arXiv:1711.03971

Agnello A., Grillo C., Jones T., Treu T., Bonamigo M., Suyu S. H., 2018, MNRAS, 474, 3391

Bade, N., Siebert, J., Lopez, S., Voges, W., & Reimers, D. 1997, AA, 317, L13

Berghea C. T., Nelson G. J., Rusu C. E., Keeton C. R., Dudik R. P., 2017, ApJ, 844, 90

Blandford R. D., Narayan R., 1992, ARA&A, 30, 311

Boller, T., Freyberg, M. J., Trümper, J., et al. 2016, AA, 588, A103

Bonvin V., et al., 2017, MNRAS, 465, 4914

Boyle B. J., Shanks T., Croom S. M., Smith R. J., Miller L., Loaring N., Heymans C., 2000, MNRAS, 317, 1014

Castander F. J., Treister E., Maza J., Gawiser E., 2006, ApJ, 652, 955

Chan, J. H. H., Suyu, S. H., Chiueh, T., et al. 2015, ApJ, 807, 138

de Jong J. T. A., et al., 2015, A&A, 582, A62

de Jong J. T. A., et al., 2017, A&A, 604, A134

Dey, A., Schlegel, D. J., Lang, D., et al. 2018, arXiv:1804.08657

Diehl H. T., et al., 2017, ApJS, 232, 15

Gaia Collaboration, et al., 2016, A&A, 595, A1

Georgakakis, A., & Nandra, K. 2011, MNRAS, 414, 992

Griffith, M. R., & Wright, A. E. 1993, AJ, 105, 1666

Inada N., et al., 2012, AJ, 143, 119

Jones D. H., et al., 2004, MNRAS, 355, 747

King, L. J., Browne, I. W. A., Marlow, D. R., Patnaik, A. R., & Wilkinson, P. N. 1999, MNRAS, 307, 225

Lang, D., Hogg, D. W., & Schlegel, D. J. 2016, AJ, 151, 36

Laureijs, R. J., Duvet, L., Escudero Sanz, I., et al. 2010, Proc. SPIE, 7731, 77311H

Lemon C. A., Auger M. W., McMahon R. G., Koposov S. E., 2017, MNRAS, 472, 5023

Lemon C. A., Auger M. W., McMahon R. G., Ostrovski F., 2018, MNRAS, tmp, 893L

Lin H., et al., 2017, ApJ, 838, L15

Mauch, T., Murphy, T., Buttery, H. J., et al. 2003, MNRAS, 342, 1117

McMahon, R. G., Banerji, M., Gonzalez, E., et al. 2013, The Messenger, 154, 35

Meisner, A. M., Lang, D., & Schlegel, D. J. 2017, AJ, 154, 161

Merloni, A., Predehl, P., Becker, W., et al. 2012, arXiv:1209.3114

Myers S. T., et al., 2003, MNRAS, 341, 1

More A., et al., 2016, MNRAS, 456, 1595

More A., et al., 2017, MNRAS, 465, 2411

Morgan N. D., Caldwell J. A. R., Schechter P. L., Dressler A., Egami E., Rix H.-W., 2004, AJ, 127, 2617

Morgan C. W., Kochanek C. S., Dai X., Morgan N. D., Falco E. E., 2008, ApJ, 689, 755-761

Muñoz, J. A., Falco, E. E., Kochanek, C. S., et al. 2001, ApJ, 546, 769

Muñoz J. A., Falco E. E., Kochanek C. S., Lehár J., Mediavilla E., 2003, ApJ, 594, 684

Oguri M., et al., 2006, AJ, 132, 999

Oguri M., Marshall P. J., 2010, MNRAS, 405, 2579

Ostrovski F., et al., 2017, MNRAS, 465, 4325

Pâris I., et al., 2017, arXiv, arXiv:1712.05029

Refsdal S., 1964, MNRAS, 128, 307

Reimers D., Koehler T., Wisotzki L., 1996, A&AS, 115, 235

Salvato, M., Buchner, J., Budavári, T., et al. 2018, MNRAS, 473, 4937

Shanks T., et al., 2015, MNRAS, 451, 4238

Schechter, P. L., Pooley, D., Blackburne, J. A., & Wambsganss, J. 2014, ApJ, 793, 96

Schechter P. L., Morgan N. D., Chehade B., Metcalfe N., Shanks T., McDonald M., 2017, AJ, 153, 219

Schechter P. L., Anguita T., Morgan N. D., Read M., Shanks T., 2018, arXiv, arXiv:1805.01939

Sluse, D., Surdej, J., Claeskens, J.-F., et al. 2003, AA, 406, L43

Suyu S. H., et al., 2013, ApJ, 766, 70

Suyu S. H., et al., 2017, MNRAS, 468, 2590

The Dark Energy Survey Collaboration, 2005, astro, arXiv:astro-ph/0510346

Dark Energy Survey Collaboration, et al., 2016, MNRAS, 460, 1270

Treu T., Marshall P. J., 2016, A&ARv, 24, 11

Vegetti S., Czoske O., Koopmans L. V. E., 2010, MNRAS, 407, 225

Vegetti S., Lagattuta D. J., McKean J. P., Auger M. W., Fassnacht C. D., Koopmans L. V. E., 2012, Natur, 481, 341

Véron-Cetty, M.-P., & Véron, P. 2003, AA, 412, 399

Williams P., Agnello A., Treu T., 2017, MNRAS, 466, 3088

Witt H. J., Mao S., Keeton C. R., 2000, ApJ, 544, 98

Wright E. L., et al., 2010, AJ, 140, 1868-1881

Walsh D., Carswell R. F., Weymann R. J., 1979, Natur, 279, 381

Warren, S. J., Cross, N. J. G., Dye, S., et al. 2007, arXiv:astro-ph/0703037

Weymann, R. J., Latham, D., Angel, J. R. P., et al. 1980, Nat, 285, 641

Wisotzki L., Koehler T., Groote D., Reimers D., 1996, A&AS, 115, 227

Wisotzki L., Christlieb N., Liu M. C., Maza J., Morgan N. D., Schechter P. L., 1999, A&A, 348, L41

York D. G., et al., 2000, AJ, 120, 1579

APPENDIX A: LIST OF HIGH-GRADED CANDIDATES

In the following tables we provide a list of high-graded lensed quasars candidates found with these searches over DES-DR1, divided by search method. The magnitudes are from WISE and Gaia-DR1 and given in the Vega system.

This paper has been typeset from a TEX/ LATEX file prepared by the author.

Table A1. List of candidates recovered by the methods based on optical colours and spectra described in Section 2.

Object Name	$W1$	$W2$	$W3$	G	Methods	Other
J000128.98-554959.1	14.93±0.03	14.17±0.04	11.85±0.23	19.39	W2MG1mult	
J005301.98+002043.2	15.13±0.04	14.02±0.05	11.75±0.34	17.65	W2MG1sing	PanSTARRS
J011455.07-054753.7	14.92±0.04	14.59±0.06	10.73±0.10	19.91	W2MG1mult	PanSTARRS
J011509.25-231453.5	14.41±0.03	14.06±0.04	11.51±0.18	19.14	W2MG1sing	PanSTARRS
J020157.21-051000.9	14.79±0.03	14.35±0.04	11.47±0.15	19.92	W2MG1sing	PanSTARRS
J021524.18-472845.0	14.41±0.03	13.33±0.03	10.04±0.05	18.60	W2MG1sing	
J023207.66-325458.1	14.95±0.03	14.59±0.05	11.76±0.18	19.13	W2MG1mult	KiDS
J023639.92-475231.6	14.06±0.03	13.31±0.03	9.95±0.05	20.13	W2MG1sing	
J030606.05-611130.0	15.22±0.03	14.78±0.04	10.61±0.07	20.31	W2MG1sing	
J033908.87-612144.7	14.61±0.03	13.44±0.03	10.26±0.05	18.45	W2MG1mult	
J035542.64-533440.3	14.31±0.03	13.56±0.03	9.92±0.03	20.23	W2MG1sing	
J040148.10-251438.0	14.17±0.03	13.12±0.03	10.20±0.06	18.79	W2MG1sing	PanSTARRS
J041848.07-275410.1	14.34±0.03	13.88±0.03	10.21±0.05	19.85	W2MG1mult	PanSTARRS
J045453.01-302636.0	14.85±0.03	14.48±0.04	11.33±0.13	18.79	W2MG1sing	PanSTARRS
J050120.31-633247.8	13.47±0.02	12.54±0.02	9.75±0.03	20.58	W2MG1sing	
J215713.63-420149.5	12.40±0.02	11.16±0.02	8.65±0.02	17.84	W2MG1sing	
J003247.75-243429.0	16.39±0.06	15.99±0.15	11.98	19.89	GaiaDR2mult	
J004254.16+045254.2	14.06±0.03	13.81±0.05	11.49	18.27	GaiaDR2mult	PanSTARRS
J005813.40-394724.6	14.77±0.03	14.05±0.04	11.23±0.12	19.42	GaiaDR2mult	PanSTARRS
J012325.25-204852.9	14.68±0.03	14.37±0.05	11.94	18.78	GaiaDR2mult	PanSTARRS
J015033.23-030746.5	15.97±0.05	14.83±0.07	11.53±0.20	20.07	GaiaDR2mult	PanSTARRS
J024754.77-634923.2	15.10±0.03	14.36±0.04	11.44±0.11	19.68	GaiaDR2mult	
J041137.60-483935.8	14.71±0.03	14.42±0.03	11.83±0.13	18.98	GaiaDR2mult	
J052611.27-393346.6	15.47±0.04	14.74±0.05	11.65±0.16	19.98	GaiaDR2mult	
J060832.98-351309.7	15.47±0.04	14.39±0.04	11.34±0.12	20.05	GaiaDR2mult	
J212034.78-423904.7	14.82±0.03	13.71±0.04	10.83±0.11	19.37	GaiaDR2mult	
J201425.41-595746.6	14.81±0.03	13.91±0.04	11.17±0.13	17.56	GaiaDR2mult	
J202649.74-422818.6	14.83±0.04	13.99±0.05	11.24±0.16	19.70	GaiaDR2mult	
J203348.67-593640.1	13.28±0.02	12.55±0.02	10.04±0.05	19.99	GaiaDR2mult	
J210014.9-445206.4	14.14±0.03	13.42±0.03	10.74±0.10	18.79	GaiaDR2mult	
J211242.15-595924.2	14.98±0.03	14.44±0.05	10.70±0.10	17.76	GaiaDR2mult	
J212354.86+004416.2	16.04±0.06	15.66±0.14	11.87	-	GaiaDR2mult	PanSTARRS
J215021.33-565008.5	16.14±0.11	15.76±0.18	11.57	20.30	GaiaDR2mult	
J215431.92-444302.0	14.63±0.03	14.35±0.05	11.68	19.18	GaiaDR2mult	
J215837.29-581203.9	14.70±0.03	13.87±0.03	11.52±0.17	19.67	GaiaDR2mult	
J220819.74-631500.9	15.00±0.03	14.70±0.06	11.66	19.31	GaiaDR2mult	
J001947.71-293255.2	16.33±0.07	16.47±0.24	12.16	-	2QZ	KiDS/PanSTARRS
J003503.89-313203.2	17.73±0.20	16.68	12.36	-	2QZ	KiDS
J023023.47-281003.3	16.54±0.07	16.00±0.14	12.60±0.42	-	2QZ	KiDS/PanSTARRS
J023221.00-314913.1	- -	- -	- -	-	2QZ	
J025001.69-373244.7	14.58±0.03	13.74±0.03	9.26±0.03	-	6dFGS	
J030403.03-195524.4	15.86±0.04	14.76±0.05	10.28±0.06	-	6dFGS	PanSTARRS
J053009.04-383734.9	15.18±0.03	14.26±0.04	9.97±0.04	-	6dFGS	

Table A2. List of candidates recovered by the methods described in Section 2, based on X-ray and Radio data.

Object Name	$W1$	$W2$	$W3$	G	Methods	Other
J002453.30-271644.0	15.53±0.04	14.82±0.07	11.96±0.33	20.21	RASS	KiDS/PanSTARRS
J004123.99-252944.9	15.16±0.04	14.76±0.06	11.66±0.20	-	RASS	PanSTARRS
J004659.57+042039.0	15.53±0.05	15.23±0.12	11.72±0.42	-	RASS	PanSTARRS
J005044.12-524856.5	14.53±0.03	13.78±0.03	11.06±0.13	20.75	RASS	
J005911.01-015544.5	15.41±0.04	15.13±0.10	11.60±0.31	-	RASS	PanSTARRS
J010515.03-625238.5	15.64±0.04	14.92±0.05	12.46±0.39	-	RASS	
J011226.92-252032.2	14.55±0.03	13.86±0.04	11.41±0.15	-	RASS	PanSTARRS
J014802.99-210841.6	16.07±0.06	15.80±0.15	12.47	-	RASS	PanSTARRS
J020807.24-183910.9	14.42±0.03	14.12±0.04	12.08	-	RASS	PanSTARRS
J021039.97-341941.8	15.34±0.04	15.03±0.07	12.23	19.41	RASS	KiDS
J021307.50-364715.5	16.16±0.05	15.95±0.13	12.31	20.70	RASS	
J023208.04-640931.6	16.13±0.05	15.92±0.10	13.11		RASS	
J023225.72-295737.1	17.43±0.15	16.03±0.14	12.51	-	RASS	KiDS/PanSTARRS
J023919.80-470108.9	16.73±0.07	15.98±0.11	11.73±0.17	-	RASS	
J030034.07-494237.4	13.76±0.02	12.73±0.02	9.89±0.05	18.09	RASS	
J032354.51-104649.3	17.75±0.18	16.83	12.14	-	RASS	PanSTARRS
J033514.21-600808.5	14.02±0.03	12.87±0.02	10.03±0.04	17.55	RASS	
J033656.27-154756.5	15.55±0.04	15.16±0.07	12.14	-	RASS	PanSTARRS
J034732.60-175324.0	15.03±0.03	14.67±0.05	11.52±0.20	-	RASS	PanSTARRS
J035546.66-214818.5	15.56±0.04	14.85±0.06	11.08±0.12	-	RASS	PanSTARRS
J043801.62-622942.9	15.85±0.04	15.46±0.07	12.58 -	-	RASS	
J044808.16-184642.3	15.36±0.04	14.44±0.05	10.58±0.07	-	RASS	PanSTARRS
J045045.35-641642.8	16.74±0.05	15.70±0.07	13.24±0.46	-	RASS	
J053248.87-391759.1	13.57±0.02	12.62±0.02	10.37±0.06	19.92	RASS	
J215029.44-020016.9	15.18±0.04	14.89±0.08	11.05±0.15	-	RASS	PanSTARRS
J225915.21-485056.2	15.50±0.04	14.83±0.06	10.81±0.11	-	RASS	
J231409.88-421549.6	13.87±0.03	12.71±0.03	9.60±0.04	-	RASS	
J235111.37-375323.5	14.79±0.03	13.77±0.04	11.57±0.19	18.86	RASS	
J055640.64-611521.3	14.76±0.03	13.82±0.03	11.58±0.10	19.50	XMMslew	
J000806.23-561551.9	16.26±0.06	15.87±0.13	11.50±0.17	-	SUMSS	
J010844.90-315335.7	14.87±0.03	14.59±0.05	12.56	-	SUMSS	KiDS
J012043.82-631556.5	13.95±0.03	12.69±0.03	9.36±0.03	-	SUMSS	
J013506.97-412612.0	11.91±0.03	11.25±0.02	6.04±0.01	17.87	SUMSS	
J020722.82-533224.1	15.72±0.04	15.21±0.06	11.71±0.17	-	SUMSS	
J022238.34-531958.2	16.07±0.05	15.64±0.09	12.23	-	SUMSS	
J025310.73-552823.2	16.13±0.05	15.75±0.09	12.07±0.23	-	SUMSS	
J032028.96-530944.7	14.80±0.03	14.50±0.04	12.87	-	SUMSS	
J035425.21-642344.5	13.12±0.02	11.95±0.02	8.30±0.02	-	SUMSS	
J042936.07-582237.5	16.05±0.03	15.71±0.05	12.24±0.15	-	SUMSS	
J043228.41-545853.8	15.59±0.03	14.82±0.04	12.76±0.24	-	SUMSS	
J044242.88-481249.5	16.12±0.05	15.70±0.09	12.75	-	SUMSS	
J045947.39-641538.9	15.39±0.03	14.84±0.04	12.84±0.35	19.76	SUMSS	
J050309.96-311652.0	15.89±0.04	15.62±0.08	12.88	-	SUMSS	
J050709.35-465931.8	16.18±0.05	15.77±0.09	12.98	-	SUMSS	
J051052.38-520129.2	15.34±0.03	14.98±0.05	12.84	19.31	SUMSS	
J053128.21-383954.3	17.91±0.18	17.50±0.44	-	-	SUMSS	
J211006.51-484121.1	16.21±0.06	15.77±0.12	12.49±0.45	-	SUMSS	
J215533.59-483645.2	16.74±0.09	16.21±0.19	12.06±0.35	-	SUMSS	
J225710.84-535824.9	15.45±0.04	15.13±0.08	12.32±0.42	19.59	SUMSS	
J222136.92-574847.6	15.10±0.04	14.44±0.04	12.20±0.33	-	SUMSS	
J233432.25-585646.7	15.71±0.04	15.41±0.09	12.32±0.42	-	SUMSS	
J234038.36-461254.8	16.27±0.06	15.66±0.11	12.17±0.33	-	SUMSS	
J234721.48-561943.7	15.46±0.04	15.17±0.06	12.42	-	SUMSS	
J234839.67-520936.5	14.61±0.03	14.10±0.04	12.10±0.34	-	SUMSS	
J235311.68-544823.3	16.80±0.09	15.84±0.13	11.96	-	SUMSS	